ICSV13 - Vienna
The Thirteenth International Congress on Sound and Vibration
Vienna, Austria, July 2-6, 2006

Reconstruction of the acoustic field using patch surface measurements

Nicolas P. Valdivia and Earl G. Williams

Acoustics Division, code 7130, Naval Research Laboratory,
Washington, DC 20375-5320, USA
valdivia@pa.nrl.navy.mil

Abstract
Near-field acoustical holography (NAH) requires the measurement of the near-field pressure field over a conformal and closed surface in order to recover the acoustic field on a nearby surface. Very often we encounter applications where pressure measurements are available only over a small open surface. In these cases the strict NAH theory does not hold, but still there are techniques used to overcome this difficulty. The best known is patch NAH, which has been used for planar surfaces. In this work we will discuss two techniques used for general surfaces: patch inverse boundary element methods (IBEM) and patch NAH using equivalent sources. We will compare the error of the normal velocity reconstruction in both methods and recommend possible improvements. We use a cylindrical surface excited by a point force as an example to validate our results.

INTRODUCTION

Denote as Γ the surface of cylinder as shown in figure 1. For a time-harmonic ($e^{-i\omega t}$) disturbance of frequency ω the sound pressure p satisfies the homogeneous Helmholtz equation inside the fuselage

$$\Delta p + k^2 p = 0, \tag{1}$$

where $k = \omega/c$ is the wave number and c the constant for the speed of sound.

The conventional solution of interior NAH will require that the pressure should be measured on a closed surface interior to Γ. Ideally this measurement surface will be very close to Γ in order to obtain a high-resolution reconstruction. However, practical implementations does not allow a closed and all encompassing measurement surface. Thus a smaller measurement surface, or "patch" surface, is used instead. In this work we will consider the case when

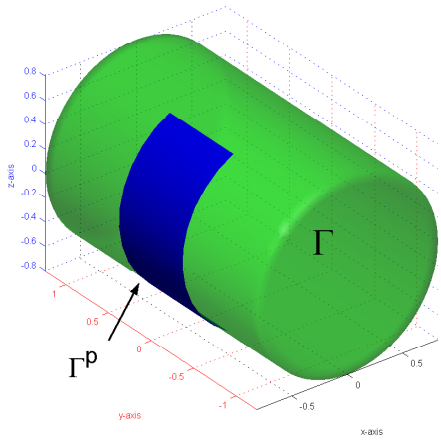

Figure 1: Cylindrical surface Γ *and the patch surface* Γ^p.

measurements are taken over a patch Γ_0, where this patch is conformal the surface Γ^p (see figure 1).

We use the integral representation[1, 2, 3] for a point $\mathbf{x} = (x_1, x_2, x_3) \in \Gamma_0$

$$p(\mathbf{x}) = \int_{\Gamma^p} \Phi(\mathbf{x}, \mathbf{y}) \varphi(\mathbf{y}) dS(\mathbf{y}), \tag{2}$$

where

$$\Phi(\mathbf{x}, \mathbf{y}) = \frac{\exp(ik\,|\mathbf{x} - \mathbf{y}|)}{4\pi\,|\mathbf{x} - \mathbf{y}|}.$$

Similarly the normal velocity is given by

$$i\rho\omega v(\mathbf{x}) = \int_{\Gamma^p} \frac{\partial \Phi(\mathbf{x}, \mathbf{y})}{\partial \mathbf{n}(\mathbf{x})} \varphi(\mathbf{y}) dS(\mathbf{y}) + \frac{1}{2}\varphi(\mathbf{x}), \quad \mathbf{x} \in \Gamma^p, \tag{3}$$

where $\mathbf{n}$ is the outward unit normal and ρ the constant of the medium density.

A solution p of (1) can be represented by the method of equivalent sources[4, 5]. In this method we are required to define a source surface Γ_s lies at a constant distance δ from Γ^p as shown in figure 2. This method uses the representation

$$p(\mathbf{x}) = \sum_{j=1}^{N_s} q_j \Phi(\mathbf{x}, \mathbf{z_j}), \quad \mathbf{z}_j \in \Gamma_s, \tag{4}$$

where $N_s > 0$ is the number of sources and $q_j, j = 1, ..., N_s$ the source coefficients. The normal derivative is calculated using

$$i\rho\omega v(\mathbf{y}) = \sum_{j=1}^{N_s} q_j \frac{\partial \Phi\left(\mathbf{y}, \mathbf{z}_j\right)}{\partial \mathbf{n}(\mathbf{y})}, \quad \mathbf{y} \in \Gamma. \tag{5}$$

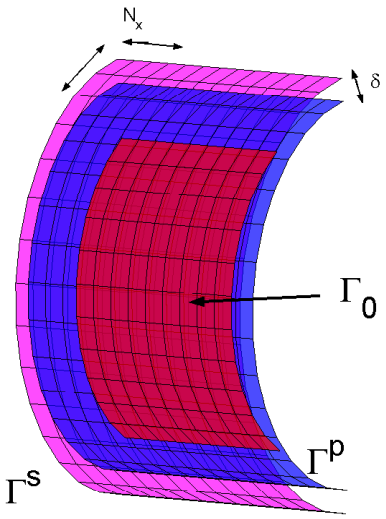

Figure 2: Surfaces Γ^p, Γ^s and Γ_0.

NUMERICAL DISCRETIZATION

The boundary surface Γ^p is decomposed into quadrilateral elements with four nodes. The boundary element method with iso-parametric linear functions[3] is selected for interpolating the geometric and acoustical quantities. Given M pressure measurements on Γ_0, represented as $\mathbf{p}$, recover N pressure and normal velocity points on Γ^p, represented as $\mathbf{p}^s$ and $\mathbf{v}^s$ respectively. When $\mathbf{x} \in \Gamma_0^p$, (2) gives the matrix equation

$$[\mathbf{S}]\,\boldsymbol{\varphi} = \mathbf{p} \tag{6}$$

where $[\mathbf{S}]$ is a $M \times N$ complex matrix and $\boldsymbol{\varphi}$ is the column vector of N entries that represent values of the density φ on Γ. Similarly, when $\mathbf{x} \in \Gamma$, (3) produce the matrix equation

$$\mathbf{v}^s = [\mathbf{K}]\,\boldsymbol{\varphi}, \tag{7}$$

where $[\mathbf{K}]$ is an $N \times N$ complex matrix.

The source surface Γ_s does not need to be decomposed into surface elements, instead we just need to create a grid with N_s points distributed over Γ^s. Then is simple to obtain the following matrix system

$$[\mathbf{G}]\,\mathbf{q} = \mathbf{p}, \tag{8}$$

where the coefficients of the $M \times N_s$ complex matrix $[\mathbf{G}]$ are given by

$$G_{ij} = \Phi(\mathbf{x}_i, \mathbf{z}_i).$$

Here $\mathbf{x}_i$ are the points in Γ_0 and $\mathbf{z}_j$ are the points in Γ_s. Similarly we obtain the relationship

$$\mathbf{v}^s = \frac{1}{i\rho\omega}\,[\mathbf{G}^{sv}]\,\mathbf{q} \tag{9}$$

where the coefficients of the $N \times N_s$ complex matrix $[\mathbf{G}^{sv}]$ are given by

$$G_{ij}^{sv} = \frac{\partial \Phi(\mathbf{y}_i, \mathbf{z}_i)}{\partial \mathbf{n}(\mathbf{y}_i)},$$

and $\mathbf{y}_i$ are the points in Γ

NUMERICAL REGULARIZATION

For the experimental problem, the exact pressure $\mathbf{p}$ is perturbed by measurement errors. We denote the measured pressure as $\mathbf{p}^m$. If the elements of the perturbation $\mathbf{e} = \mathbf{p}^m - \mathbf{p}$ are Gaussian (unbiased and uncorrelated) with covariance matrix $\sigma_0^2 [\mathbf{I}]$, then $E\left(\|\mathbf{e}\|_2^2\right) = M\sigma_0^2$ (here $\|.\|_2$ is the 2-norm). It is well known that the linear systems on (6) and (8) are ill-posed, i.e., the errors in $\mathbf{p}^m$ will be amplified in the solution $\boldsymbol{\varphi}$ or $\mathbf{q}$, and in most of the cases the recovery will be useless.

To avoid the amplification of the measurement errors, special *regularization methods* are used to find the solution of these linear systems. The best known implementation of these methods requires the use of the singular value decomposition (SVD)

$$[\mathbf{S}] = \left[\mathbf{U}^1\right] \left[\mathbf{\Sigma}^1\right] \left[\mathbf{V}^1\right]^H, \quad [\mathbf{G}] = \left[\mathbf{U}^2\right] \left[\mathbf{\Sigma}^2\right] \left[\mathbf{V}^2\right]^H$$

where $\left[\mathbf{U}^{1,2}\right]$, $\left[\mathbf{V}^{1,2}\right]$ are unitary matrices and $\left[\mathbf{\Sigma}^{1,2}\right]$ is a diagonal matrix containing the singular values σ_i in order of non-decresing magnitude. Regularization methods are implemented using the explicit formula

$$\boldsymbol{\varphi}_\alpha = \left[\mathbf{V}^1\right] \left[\mathbf{F}^{1,\alpha}\right] \left[\mathbf{\Sigma}^1\right] \left[\mathbf{U}^1\right]^H, \quad \mathbf{q}_\alpha = \left[\mathbf{V}^2\right] \left[\mathbf{F}^{2,\alpha}\right] \left[\mathbf{\Sigma}^2\right] \left[\mathbf{U}^2\right]^H, \tag{10}$$

Here the diagonal matrices $\left[\mathbf{F}^{1,\alpha}\right], \left[\mathbf{F}^{2,\alpha}\right]$ contain the filter factors[6] which are used to reduce the effect of the measurement errors in the reconstruction. The parameter $\alpha \geq 0$ is called the regularization parameter, and should be chosen correctly. There are several types of filter factors used for different ill-posed problems, but in this work we will use the filter factors of Tikhonov with a high-pass filter[7].

PHYSICAL EXPERIMENTS

The experimental configuration for the holographic measurement is similar to the previous work of Herdic[8]. The surface Γ is an aluminium stiffened cylindrical shell (0.81m radius, 2.55m length and the shell thickness varies between 0.8 and 1.2mm) excited by a point force applied to a rib/stringer intersection at one end of the cylinder. The measurements were conducted using a chirp waveform over a band from 10 to 1000Hz with 0.61Hz resolution. For this interior NAH problem, the measurement surface Γ_0 is a cylindrical array of 0.7045m radius, 123.75 degrees angle and 0.74m length as shown in figure 2. The pressure measurements on Γ_0 are a grid of 12 points over the radius and 10 points over the length.

Γ^p is a patch of the surface Γ that is directly in front of Γ_0. Γ^p is a cylindrical surface of 0.81m radius, with the same angle and length than Γ_0. The normal velocity is measured over 120 points in Γ^p distributed as in Γ_0. We will consider the use of extension points N_x in Γ^p (and Γ^s for ESM), which will make the cylindrical surface angle $146.25, 168.75$ degrees and respectively the length $0.91, 1.08$m for $N_x = 1, 2$ (see figure 2).

The vector $\mathbf{v}^s$ contain the measured normal velocity on Γ^p with $N_x = 0$. Notice that the previous methods will provide the reconstructed normal velocity $\mathbf{v}_r^s$ for Γ^p (even over extended points $N_x > 0$), but the relative error $\|\mathbf{v}^s - \mathbf{v}_r^s\|_2/\|\mathbf{v}^s\|_2 \times 100$ will be considered over the part of Γ^p that was not extended ($N_x = 0$). Since we know the exact $\mathbf{v}^s$, we choose in all our reconstructions the optimal regularization parameter α for the Tikhonov regularization with a high-pass filter in (10).

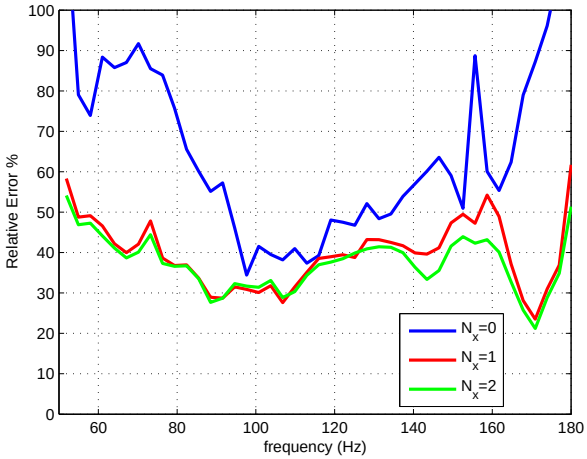

Figure 3: Patch IBEM reconstruction for different frequencies using extension points N_x.

In figure 3 we show the relative error of reconstructed normal velocity using patch IBEM for 44 frequencies equally spaced from 88.5Hz to 180Hz. This figure clearly shows the importance of the extension points. When $N_x = 0$ the errors are bigger for all frequencies. $N_x = 1, 2$ have similar errors, but $N_x = 2$ does slightly better. If we utilize more extension points we will observe that the errors will not decrease, but instead the columns of the matrix system in (7) will increase. The increase in the columns of the matrix $[\mathbf{S}]$ in (7) will increase considerably the memory requirements of patch IBEM. For that reason is just necessary to use $N_x = 2$ with patch IBEM.

In figure 4 we show the relative error of the reconstructed normal velocity using ESM with $\delta = 0.08$m for 44 frequencies equally spaced from 88.5Hz to 180Hz. This figure shows that the reconstruction errors are similar to the reconstruction errors of patch IBEM for different extension points. When $N_x = 0$ the errors are higher for all frequencies, and for $N_x > 0$ the errors reduce. Again as for the patch IBEM method, there will not be a considerable decrease in the reconstruction point for N_x greater than 2.

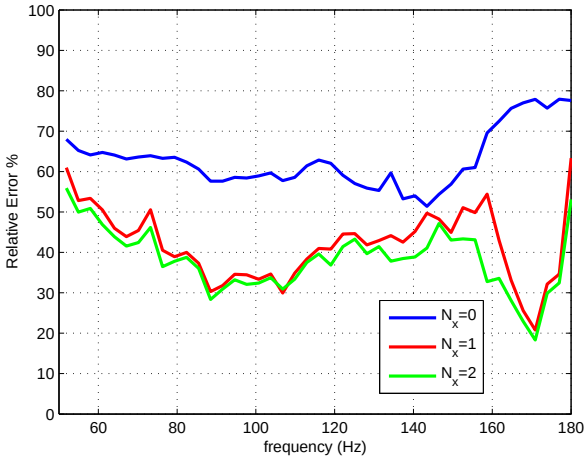

Figure 4: ESM with $\delta = 0.08$m reconstruction for different frequencies using extension points N_x.

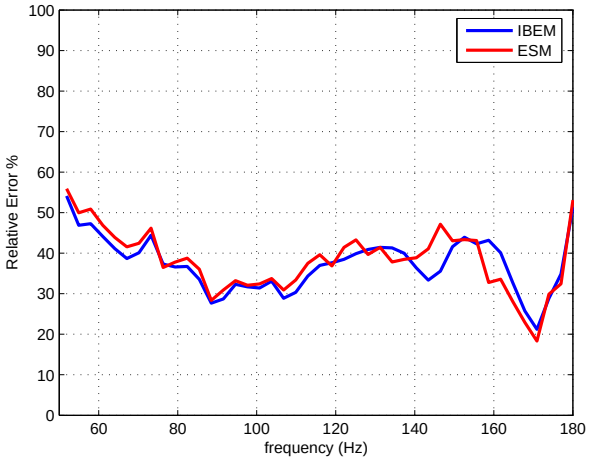

Figure 5: patch IBEM and ESM reconstruction for different frequencies using extension point $N_x = 2$.

In figure 5 we show the comparison between the errors of patch IBEM and ESM with $\delta = 0.08$m. In both methods we use $N_x = 2$ and we found that they produce similar errors for all frequencies. Finally in figure 6 we show the normal velocity measurements $\mathbf{v}^s$ in Γ^p and in figure 7 we show the reconstructed normal velocity $\mathbf{v}_r^s$ using patch IBEM with extension points $N_x = 2$.

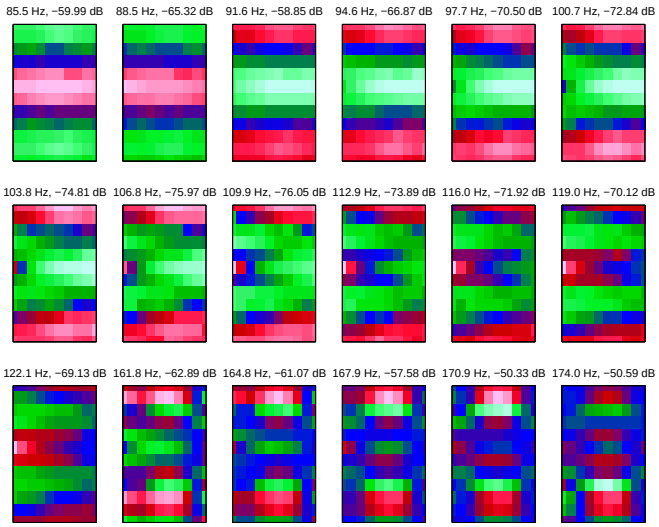

Figure 6: Normal Velocity measurements for some selected frequencies.

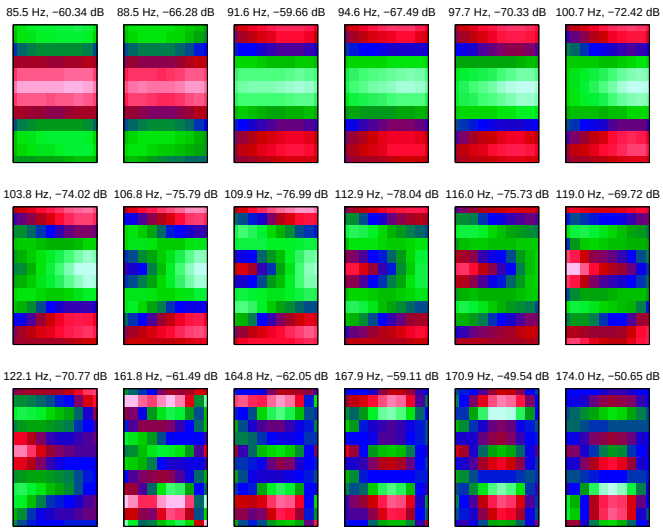

Figure 7: Normal Velocity reconstruction using patch IBEM with extension points $N_x = 2$ for some selected frequencies.

CONCLUSION

In this work we have shown two methods that are used for the reconstruction of the normal velocity when measurements are available over a patch: patch IBEM and ESM. It was found that both methods produce similar reconstruction errors, and also in both methods these errors can be reduced by the use of extension points in the reconstruction surface Γ^p (and source surface Γ^s for ESM).

ESM does not require the time-expensive calculations of the integral as in IBEM. For that reason we have shown that ESM can be numerically more attractive than patch IBEM, when patch measurements are available.

ACKNOWLEDGEMENTS

This work was supported by the Office of Naval Research.

REFERENCES

References

[1] D. Colton, R. Kress, *Integral Equation Methods in Scattering Theory*, Wiley-Interscience Publication, New York, NY (1983).

[2] T. K. DeLillo, V. Isakov, N. Valdivia, L. Wang, *The detection of surface vibrations from interior acoustical pressure*, Inverse Problems., 19(3), (2003), 507–524.

[3] N. Valdivia, E. G. Williams, *Implicit methods of solution to integral formulations in boundary element methods based near-field acoustic holography*, J. Acoust. Soc. Am., 116(3), (2004), 1559–1572.

[4] A. Sarkissian, *Extension of measurement surface in near-field acoustic holography*, J. Acoust. Soc. Am., 115, (2004), 1593–1596.

[5] A. Sarkissian, *Method of superposition applied to patch near-field acoustic holography*, J. Acoust. Soc. Am., 118, (2005), 671–678.

[6] P. C. Hansen, *Rank-Deficient and Discrete Ill-Posed Problems*, Siam, Philadelphia, PA (1998).

[7] E. G. Williams, *Regularization methods for near-field acoustical holography*, J. Acoust. Soc. Am., 110, (2001), 1976–1988.

[8] P. Herdic, B. Houston, M. Marcus, E. Williams, A. Baz, *The vibro-acoustic response and analysis of a full-scale aircarft fuselage section for interior noise reduction*, J. Acoust. Soc. Am., 117, (2005), 3667–3678.